DEET Degradation by Titanium Dioxide–Zeolite Nanocomposites: Effects of Aggregation State, Water Chemistry, and Natural Organic Matter

Tchemongo B. Berté,[1,†] Anthony S. Chen,[1,†] Riya A. Mathew,[1] Sheyda Shakiba,[1] and Stacey M. Louie[1*]

[1]Department of Civil & Environmental Engineering,

University of Houston, Houston, TX 77004, United States

[†] Equal contribution

[*]Corresponding author:

Phone: 713-743-8646

Fax: 713-743-4260

Email: slouie@uh.edu

Abstract

Immobilization of titanium dioxide nanoparticles (TiO_2 NPs) facilitates their removal and reuse in water treatment applications. Composite materials of electrostatically-bound TiO_2 NPs and zeolite particles have been proposed, but limited mechanistic studies are available on their performance in complex media. This study delineates the relative importance of homo- and heteroaggregation, water chemistry, and surface fouling by natural organic matter (NOM) on the photocatalytic degradation of diethyltoluamide (DEET) by TiO_2-zeolite composites. Zeolite adsorbs a portion of the DEET, rendering it unavailable for degradation; corrections for this adsorption depletion allowed appropriate comparison of the reactivity of the composites to the NPs alone. The TiO_2-zeolite composites showed enhanced DEET degradation in moderately hard water (MHW) compared to deionized water (DIW), likely attributable to the influence of HCO_3^-, whereas a net decline in reactivity was observed for the TiO_2 NPs alone upon homoaggregation in MHW. The composites also better maintained reactivity in the presence of NOM in MHW, as removal of Ca^{2+} onto the zeolite mitigated fouling of the TiO_2 surface by NOM. However, NOM induced partial dissociation of the composites. DEET byproduct formation, identified by quadrupole–time of flight (QTOF) mass spectrometry, was generally unaffected by the zeolite, while NOM fouling favored de-ethylation over hydroxylation products. Overall, the most significant factor influencing TiO_2 reactivity toward DEET was NOM adsorption, followed by homoaggregation, electrolytes (here, MHW versus DIW), and heteroaggregation. These findings can inform a better understanding of NP reactivity in engineered water treatment applications.

Introduction

Advanced oxidation processes, such as photocatalysis, are of high interest to degrade emerging contaminants such as pesticides and pharmaceuticals that are commonly detected in surface waters but may not be removed in traditional drinking water treatment processes.[1] One of the most widely studied photocatalysts is titanium dioxide (TiO_2) nanoparticles (NPs), which are attractive for their low aqueous solubility and ready availability. However, the use of TiO_2 NP suspensions as-is presents several challenges in both research and application. Separation of the NPs from treated water can require costly centrifugation or filtration processes, limiting their feasibility for water treatment operations. The NPs are also prone to aggregate, hampering the efficiency of the advanced oxidation process[2-5] and reusability of the NPs. Homoaggregation also complicates research studies seeking to fundamentally compare NP reactivity under different conditions (e.g. water chemistries), if the aggregation cannot be controlled across all conditions.[6]

One strategy to address these challenges is immobilization of the NPs onto a fixed or easily removable substrate to form a composite material.[1,7-9] The selection of the immobilization method and support material will determine the robustness of the composite (i.e. resistance to decomposition or loss of TiO_2 that would result in a poorer capacity for recycling or reuse) and can also influence pollutant removal. Several support materials have been tested, including silica,[10] activated carbon,[11,12] and hydrogels,[13] with sorptive substrate materials serving for additional removal or to enhance the pollutant concentration near the TiO_2 for higher degradation rates.[7]

Zeolites are microporous, aluminosilicate materials, traditionally used as an adsorbent,[14] that have also been widely investigated as a low-cost support for TiO_2 NPs for water treatment or vapor-phase contaminant removal.[2,10,15-20] Several immobilization approaches can be taken, including sol-gel synthesis of TiO_2[12,17,20] or wet incipient impregnation[16,17,19] followed by

calcination onto the TiO_2. In this study, we apply an alternative approach reported in a patent by the Panasonic Corporation,[21] in which TiO_2 NPs are mixed with zeolite at a pH below the isoelectric point of the TiO_2 NPs ($\approx$ 7), such that the positively-charged TiO_2 NPs attach to the negatively-charged zeolite particles by electrostatic attraction. While these materials are likely less robust to dissociation, the elimination of chemical syntheses or post-treatments such as calcination reduces material and energy costs and makes the synthesis more broadly accessible. The use of electrostatically-bound composites also allows a high photocatalytic efficiency of the TiO_2 NPs to be maintained, compared to composites prepared with binders such as silica that overcoat the reactive TiO_2 surface area.[21] Finally, preparing the composites from pre-synthesized TiO_2 NPs and zeolite stock materials allows for more controlled studies, in which each component can easily be compared alone or together in the composite to evaluate the effects of immobilization.

Despite TiO_2-zeolite composites being widely studied, limited mechanistic studies are available on the influence of the zeolite substrate on contaminant removal. Prior studies focused on the role of the hydrophobicity of the zeolite,[17] the Si/Al ratio,[16] or adsorption onto the zeolite.[2] In cases where adsorption to zeolite occurred, compensation for the adsorption was not made in order to assess photocatalysis by the TiO_2 separately from the adsorptive removal. In addition, the composites have not yet been evaluated across a range of water chemistries, e.g. different pH, electrolyte composition, or the presence of natural organic matter (NOM). In these complex media, the performance of the NPs can be influenced by changes in their aggregation state, as well as interactions of the substrate with the contaminant or other aqueous constituents. Another limitation in prior studies is that probe compounds for degradation have typically been charged (cationic/anionic) or weak acid/base compounds, where the influence of water chemistry is dominated by changes in adsorption at different pH spanning either the isoelectric point of the

TiO_2 NPs or the pK_a of weak acid or base groups on the target compound,[22-25] obscuring other possible effects of water chemistry on the surface reactivity of the NPs. Finally, the formation of degradation byproducts is not typically evaluated, but this analysis is necessary to identify whether reaction pathways are influenced by immobilization or by the water chemistry. In summary, additional studies are needed that systematically evaluate each of the possible influences of the substrate and water chemistry on the performance of immobilized TiO_2 NPs for water treatment.

The objective of this research is to provide a thorough analysis of the role of the zeolite substrate and water chemistry, including fouling by NOM, on the photocatalytic efficiency of TiO_2 NPs for removal of a model pesticide, diethyltoluamide (DEET). DEET is an uncharged compound whose adsorption to TiO_2 does not vary substantially with the NP surface charge, allowing a more fundamental understanding of NP reactivity separately from adsorption effects. The TiO_2-zeolite composites are compared to TiO_2-only and zeolite-only suspensions to fully elucidate the role of the zeolite support on the DEET removal in deionized water (DIW) and moderately hard water (MHW) with or without NOM. DEET degradation was evaluated using high performance liquid chromatography (HPLC) with UV detection for quantification and quadrupole–time of flight mass spectrometry (QTOF MS) for byproduct identification. Dynamic light scattering (DLS) and sedimentation experiments were used to evaluate the TiO_2 or composite aggregation state, and size exclusion chromatography (SEC) was used to investigate the influence of the zeolite substrate on NOM adsorption. The set of experimental conditions and suite of characterization methods applied in this study enable the relative importance of several factors (homoaggregation, heteroaggregation, water chemistry, and NOM adsorption) to be distinguished.

Materials and Methods

Chemical Reagents

TiO_2 NPs (Aeroxide P25, Evonik Industries, Essen, Germany) and zeolite (Zeolite Y, hydrogen, Si:Al molar ratio = 30:1, Alfa Aesar, Haverhill, MA) were used to prepare the TiO_2-zeolite composites and suspensions of the individual materials. DEET (PESTANAL analytical standard, Sigma-Aldrich, Burlington, MA) was used as the model contaminant. Suwannee River natural organic matter (SRNOM, International Humic Substances Society, St. Paul, MN), $CaCl_2$ (> 97.0%, anhydrous, ACS grade, Sigma-Aldrich), $NaHCO_3$ (> 99.7%, ACS grade, Sigma-Aldrich), and deionized (DI) water (Modulab Water Systems, Evoqua, Pittsburgh, PA) were used to prepare the background matrices. HPLC solvents were prepared using LC-MS grade water (OmniSolv LC-MS, MilliporeSigma), LC-MS grade acetonitrile (≥ 99.9%, OmniSolv LC-MS, MilliporeSigma), and formic acid (ACS reagent, Honeywell, Charlotte, NC). HCl (ACS reagent, Sigma-Aldrich) and NaOH (Sigma-Aldrich) were also used.

Preparation of Particle Stock Suspensions

TiO_2 NP stock suspensions and acid-washed zeolite particles were prepared following the dispersion and processing protocols reported by the National Institute of Standards and Technology (NIST)[26] and Panasonic,[21] respectively. The full dispersion procedures, including any modifications to the reference protocol, are provided in the Supplementary Information (SI).

The TiO_2-zeolite composites were also prepared following the procedures reported by Panasonic.[21] A mixture comprised of 0.9 g/L of TiO_2 particles and 2.7 g/L of zeolite was prepared in DI water from the stock TiO_2 suspension and acid-processed zeolite particles, with a resulting pH of 3.8 due to residual acids on the TiO_2 and/or zeolites. The TiO_2-zeolite suspension was bath

sonicated for 60 min and then stirred for 60 min with a magnetic stirrer at 300 rpm to encourage heteroaggregation.[21] The composite suspensions were stored in amber bottles at 4 °C. It is noted that suspensions were stored for ≈ 4 months prior to use, and additional heteroaggregation may have occurred over the storage duration.

Suspension Preparations for Photocatalysis and Characterization Experiments

Suspensions of 0.2 g/L of TiO_2 alone, 0.6 g/L of zeolite alone, or 0.8 g/L total solids of the TiO_2-zeolite composites (i.e., 0.2 g/L of TiO_2 attached to 0.6 g/L of zeolite) were used in all experiments and measurements described hereafter. Four background water chemistries were evaluated: DI water, a simplified moderately hard water (MHW) comprised of 0.85 mM $CaCl_2$ and 1.2 mM $NaHCO_3$,[27] MHW with 10 mg/L of NOM, and MHW with 50 mg/L of NOM. These NOM concentrations produced significantly different adsorbed masses on the TiO_2 in our prior study[27] and here. The initial DEET concentrations used were 50 mg/L for all particle types, as well as 100 mg/L for the zeolite and composite materials to result in a free DEET concentration of ≈ 50 mg/L after accounting for DEET adsorption to the zeolites (*vide infra*).

Characterization of Particle Size, Sedimentation Rates, and Zeta Potential

The hydrodynamic size of the TiO_2 NP suspensions noted above was measured by DLS (Zetasizer Nano ZS, Malvern Instruments, Malvern, UK) at the end of the photoreaction experiments (described below) to evaluate NP homoaggregation in the various water chemistries under both UV-exposed and dark conditions. The zeolite particles were beyond the upper size range for DLS measurement. Furthermore, settling rates were evaluated on all samples at the concentrations noted above by monitoring turbidity over time (Hach 2300 Tungsten Lamp

Turbidimeter, Loveland, CO) for 2.5 h starting immediately after the particles were added into the background water chemistry of interest. Differences in the settling rate of the different particle types serve as evidence of homoaggregation or heteroaggregation.[28] All particle samples were also characterized for zeta potential by electrophoretic light scattering (Zetasizer Nano ZS, Malvern Instruments), using folded zeta capillary cells (DTS 1070, Malvern) for measurement and the Smoluchowski fitting model to determine zeta potential from the electrophoretic mobility.

DEET Adsorption Isotherms

Adsorption of DEET to the zeolite-containing samples was measured on aqueous mixtures of 50, 100, 150, 200, 250, and 300 mg/L DEET with 0.6 g/L of zeolite or 0.8 g/L of TiO_2-zeolite composites (containing 0.6 g/L of zeolite). Samples were rotated end-over-end at 25 rpm for 1 h (the duration of the photoreaction experiments) and centrifuged at 13,000 rpm (11,337 *g*) for 15 min to pellet the particles (MiniSpin Plus, Eppendorf, Hauppauge, NY). The remaining DEET concentration in the supernatant was measured by HPLC with UV detection as described below.

UV Photocatalysis Experiments

15 mL of each sample type (TiO_2-only, zeolite-only, TiO_2-zeolite composites, and no-particle control) was added to quartz photoreactor vials, with one vial per sample uncovered and a second vial wrapped in aluminum foil to serve as a dark control. A UV reactor (Rayonet RMR-600, Southern New England Ultraviolet Co., Branford, CT) was used for irradiation, with a fan for cooling and eight UV lamps (350 nm average wavelength) surrounding a "merry-go-round" rotator with eight sample positions. The UV intensity was 5.0 ± 0.2 mW/cm^2 (n = 3 replicates), as measured by a UV AB light meter (UV513AB, GeneralTools, New York, NY) placed at the sample

position and collecting measurements over a 30 s averaging period while rotating. UV and dark (foil-wrapped) samples were placed alternately around the sample holder and rotated to achieve symmetrical exposure of the irradiated samples. 1.5 mL was withdrawn from the UV-exposed samples at 0, 2, 5, 10, 15, 30, 45 and 60 min. Controls (dark or particle-free samples) were collected at 0, 5, 15, 30, and 60 min. Before each sample collection, the vials were inverted several times to obtain a homogeneous mixture for sampling and to resuspend any settled particles. The pH of the samples was measured before and after the experiment, and the hydrodynamic size of the TiO_2 NPs was measured at the end of the experiment on the UV-exposed and dark samples to evaluate homoaggregation (zeolite particles were beyond the upper size range for DLS measurement).

All collected samples were centrifuged at 13,000 rpm (11,337 *g*) for 15 min to pellet the TiO_2 and zeolites (Eppendorf MiniSpin Plus), then filtered using a 0.2 μm nylon syringe filter (4 mm diameter, MicroSolv Technology, Leland, NC) to remove any remaining particles. The filtered samples were analyzed by HPLC-UV-QTOF for DEET quantification and byproduct analysis, as detailed below. The NOM-containing filtrates were also evaluated by SEC to quantify and characterize the NOM adsorption to the three particle types.

HPLC-UV-QTOF Measurements

Samples were analyzed on an HPLC system (1260 Infinity II, Agilent Technologies, Santa Clara, CA) comprised of a binary pump, autosampler, Zorbax Eclipse Plus C_{18} Rapid Resolution HD column (2.1 × 50 mm, 1.8 μm), and UV-Vis diode array detector, and a QTOF MS (Agilent 6545) with an electrospray ionization source (Agilent DualJet AJS). Solvents used were LC-MS grade water with 0.1% formic acid (A) and LC-MS grade acetonitrile (B). A gradient elution was run from 98% A / 2% B to 5% A / 95% B over 1 to 21 min elution time. The sample injection

volume was 1 μL. The UV absorbance at 248 nm was used for DEET quantification against external calibration standards, and the QTOF was used to identify and confirm byproduct species to compare across particle types and water chemistries. A check tune was run prior to each batch of samples, and reference mix was continually introduced during the sample measurement for TOF calibration (details in the SI). All samples were run in All Ions mode (i.e., MS scan mode with no precursor selection on the quadrupole and the collision energy cycling between 0, 10, 20, and 40 eV), using the source parameters in SI Table S1. The MS data were processed in the Agilent MassHunter Qualitative Analysis software (version 10.0) by molecular feature extraction to identify compounds and their *m*/*z* values, followed by molecular formula generation to assign putative compound formulas to the high-resolution accurate-mass data. Fragmentation patterns for the byproducts were extracted from the All Ions data. To minimize the appearance of background fragment ions, the spectrum at each collision energy was taken at the peak maximum in the extracted ion chromatogram for the precursor ion of interest, and the corresponding background spectrum taken in the chromatogram prior to the precursor peak was subtracted.

NOM Adsorption and Calcium Depletion Measurements

The NOM-containing samples from the UV and dark photoreaction experiments were also analyzed by SEC on an Agilent 1290 HPLC system with a Superdex 75 10/300 GL SEC column (GE Healthcare, Chicago, IL) and Agilent 1260 UV-Vis diode array detector set to monitor the 280 nm wavelength. The mobile phase was 4 mM phosphate buffer (pH 7) with 25 mM NaCl, and the injection volume was 100 μL. The NOM collected from the dark samples was taken to represent the NOM remaining after adsorption to the particles, while NOM collected after UV exposure was used to assess NOM and DEET degradation. Unreacted NOM standards were also

measured at the two concentrations used (10 mg/L and 50 mg/L) in MHW, with or without DEET, for comparison against the degraded samples and to assess whether any DEET-NOM complexation interactions occur that could affect the measurements or the photocatalysis reactions.

To investigate the influence of Ca^{2+} on the NOM adsorption, NOM samples were prepared with the three particle types (TiO_2 NPs, zeolite, or TiO_2-zeolite composites) as above, except replacing the 0.85 mM of $CaCl_2$ in the MHW with 1.7 mM of NaCl (i.e. the same cation charge equivalents) and allowing 1 h end-over-end sample rotation (25 rpm) without UV exposure for adsorption. Finally, the role of Ca^{2+} was further explored in Ca^{2+} adsorption experiments. Particles were prepared as above in MHW (without NOM), rotated for 1 h, and centrifuged as above to pellet the particles. The supernatant was measured with a calcium ion selective electrode (Oakton EW-27504-06, Cole-Parmer, Vernon Hills, IL) to determine the remaining dissolved Ca^{2+} concentration and calculate adsorption to the particles.

Results and Discussion

Adsorption of DEET onto Zeolite Particles or TiO_2-Zeolite Composites

To compare DEET adsorption by the zeolite particles and TiO_2-zeolite composites, batch adsorption experiments were conducted. After mixing the DEET and particles for ≈ 1 h and separating the particles, the concentration of DEET was measured by HPLC-UV. The adsorbed mass of DEET, q (mg DEET/g zeolite), was obtained by subtracting the equilibrium DEET concentration, C_e (mg/L), from the initial DEET concentration and dividing by zeolite concentration (0.6 g/L). The adsorption isotherms were fitted to a Langmuir model:

$$q = \frac{q_{\max} K C_e}{1 + K C_e} \quad (1)$$

where q_{max} (mg/g) and K (L/mg) are the maximum adsorbed capacity (assuming no multilayer adsorption) and Langmuir isotherm constant, respectively. These parameters were fitted by minimizing the sum of square errors between the Langmuir model and the experimental data.

As Figure 1 shows, both particle types reached saturation at similar DEET concentrations of (97.0 ± 2.9) mg DEET/g zeolite (n = 2 replicates) for the zeolite particles, and (93.0 ± 1.2) mg DEET/g zeolite (n = 2 replicates) for the composites. This similar DEET adsorption onto the zeolite particles and TiO_2-zeolite composites suggests no significant enhancement or blocking effect of TiO_2 in the composites. In addition, no adsorption of the DEET to the TiO_2 alone was observed over the course of an hour in dark (control) photoreactor experiments (SI Figure S1).

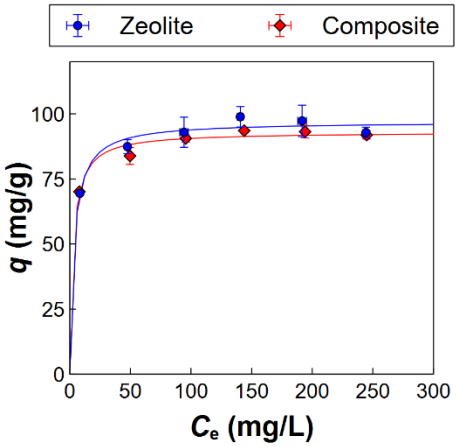

Figure 1. Adsorption isotherm of DEET onto zeolite particles or TiO_2-zeolite composites. Samples were prepared with initial concentrations of (50, 100, 150, 200, 250, and 300) mg/L of DEET and 0.6 g/L of zeolite or 0.8 g/L of TiO_2-zeolite composites (0.2 g/L TiO_2 + 0.6 g/L zeolite). Samples were mixed for 1 h and centrifuged to pellet the particles. The DEET concentration in the supernatant, C_e, was measured by HPLC with UV detection. Error bars represent the standard deviation of n = 2 experiments.

DEET Removal Rates for TiO_2 NPs and TiO_2-Zeolite Composites in Different Water Chemistries

Here, we present the overall results for the DEET degradation with the various materials, which will be followed by discussion of the mechanisms for the results in the different water chemistries in the subsequent sections. The photocatalytic degradation of DEET by the TiO_2, zeolite, and TiO_2-zeolite composites in different backgrounds (DIW, MHW, and MHW with 10 mg/L of NOM or 50 mg/L of NOM) was evaluated in the UV photoreactor. To attain a consistent initial concentration of dissolved DEET of ≈ 50 mg/L across all experiments, samples with TiO_2 alone were prepared with a total concentration of 50 mg/L of DEET (showing no measurable adsorption to the TiO_2) whereas samples containing zeolite were prepared with 100 mg/L of total DEET (resulting in ≈ 50 mg/L of free DEET after adsorption to the zeolites in Figure 1).

The irradiated TiO_2 and TiO_2-zeolite composites showed significant DEET removal (Figure 2, SI Table S2), while samples without TiO_2 (zeolite only or particle-free) and dark controls showed minimal changes in the DEET concentration, i.e. no degradation and no further adsorption over time (SI Figure S1). The initial pH of the samples was 6.1 to 6.5 in DIW and 7.8 to 8.2 in MHW with or without NOM. The pH of all UV-irradiated, TiO_2-containing samples decreased over the 60 min exposure (by ≈ 0.4 to 0.5 pH units for the TiO_2 alone in either DIW or MHW, 0.2 for the composites in MHW, and ≈ 1 for the composites in DIW), suggesting formation of acidic reaction products over time. Initial DEET removal rates (Figure 2c, SI Table S2) were obtained as the slope of the best-fit line through the first three time points up to 5 min (SI Figure S2), after which deviations from linearity were observed, likely attributable to accumulation of reaction byproducts that compete with DEET during the reaction. Comparing across water chemistries, the TiO_2 NPs showed higher reactivity in DIW compared to MHW, while the composites showed an opposite trend, i.e. a higher DEET removal rate in MHW than in DIW. The

presence of NOM suppressed the reactivity of both the TiO_2 and the composite; however, the relative degree of suppression was higher for the TiO_2 NPs than for the composite (SI Table S2**)**.

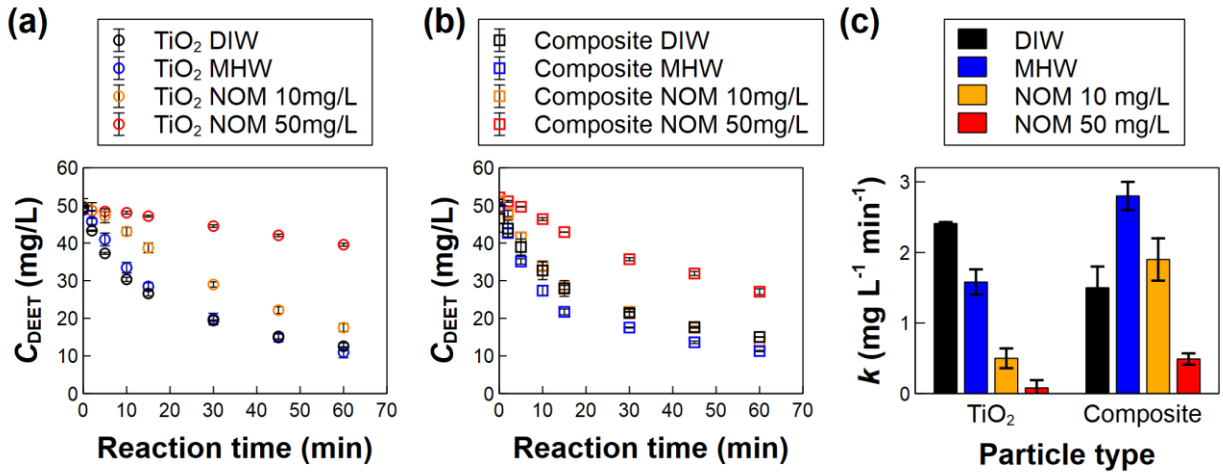

Figure 2. DEET concentration with UV exposure time using 0.2 g/L of TiO_2 NPs (a) and 0.8 g/L of TiO_2-zeolite composites (0.2 g/L TiO_2 + 0.6 g/L zeolite) (b), and pseudo-first-order decay rate constants (c). Samples were tested in DIW, MHW, and MHW with 10 mg/L or 50 mg/L of NOM. The TiO_2-only samples contained 50 mg/L of DEET, and the composite samples contained 100 mg/L of total DEET (50 mg/L of free DEET, after accounting for adsorption to the zeolites). Error bars represent the standard deviation of at least two replicate experiments.

Photocatalysis by TiO_2 is generally reported to proceed by a heterogeneous reaction at the surface of the NPs and can be described by a Langmuir-Hinshelwood model, which includes both a decay rate constant and an adsorption constant for the target compound onto the TiO_2.[29-31] Because of this dependence on the adsorbed amount, the decay rate depends on the solution-phase concentration, e.g. as in a Langmuir adsorption isotherm. Indeed, while a pseudo-first-order decay model could be fitted through the DEET degradation data (SI Figure S3, SI Table S3), the decay

rate "constant" depends significantly on the DEET solution concentration in trials comparing the composite with 50 mg/L of total DEET added (9 mg/L of free DEET remaining) to the composite with 100 mg/L of total DEET (50 mg/L of free DEET) (SI Table S2). This dependence on initial dissolved concentration indicates the reaction is not a true first-order reaction. Hence, adjusting the starting concentrations to account for the removal onto the zeolite is important to ensure decay rates are appropriately compared between the TiO_2 NPs and composite materials.

Mechanisms Influencing Reactivity in Media Without NOM: Aggregation State and Electrolytes

To explain the results observed in DIW and MHW (without NOM) in Figure 2, we hypothesized that several factors could be important, including the water chemistry (pH, electrolytes) and the aggregation state (homo- or heteroaggregation) of the NPs. The heteroaggregation state of the composite material and the homoaggregation of the TiO_2 NPs are prone to vary with water chemistry. Therefore, the particle charge was evaluated by measuring the zeta potential (Figure 3), and the aggregation state was assessed by DLS for the TiO_2 NPs and sedimentation experiments for all particles (Figure 4). The TiO_2 NPs are positively charged and zeolite is negatively charged in DIW (pH ≈ 6.5, below the isoelectric point of the TiO_2 NPs[26]). The near-neutral overall charge of the composites is hence indicative of the expected heteroaggregation of the TiO_2 onto the zeolite by electrostatic attraction (Figure 3). In DIW, both the TiO_2 NPs and zeolite particles are colloidally stable (minimal sedimentation in DIW; z-average diameter, d_z, of 167 nm for TiO_2 NPs after 1 h of either UV exposure or in the dark, compared to an initial d_z of 151 nm; zeolite size out of range for DLS measurements). Hence, the significantly faster sedimentation of the composite particles (Figure 4) is also indicative of heteroaggregation to form particles with larger overall size and higher density than the TiO_2 or zeolite alone.

The lower reactivity of the composites than the TiO_2 NPs in DIW (Figure 2) suggests that heteroaggregation reduces the reactivity of the TiO_2. This reduction in efficiency could be attributable to the lesser available surface area of TiO_2 after heteroaggregation, scattering of light by the zeolite resulting in lower UV intensity reaching the TiO_2, or mass transfer limitations.[7] Previously, only a 5% loss of efficiency was reported for the degradation of diclofenac using the TiO_2-zeolite composite relative to TiO_2 NPs alone, but with a higher overall catalyst concentration and constant stirring,[21] suggesting mass transfer limitations may be more important here.

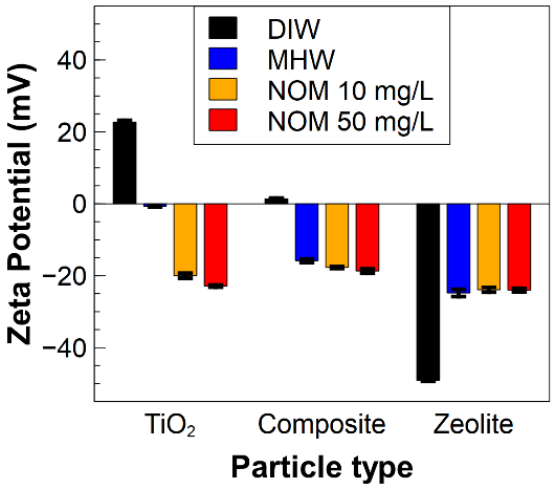

Figure 3. Zeta potential of the TiO_2 NPs (0.2 g/L), zeolite (0.6 g/L), and TiO_2-zeolite composites (0.2 g/L TiO_2 + 0.6 g/L zeolite) across different backgrounds (DIW, MHW, and MHW with 10 mg/L or 50 mg/L of NOM). The TiO_2-only samples contained 50 mg/L of DEET, and the zeolite and composite samples contained 100 mg/L of total DEET (50 mg/L of free DEET, after accounting for adsorption to the zeolites). Samples were equilibrated for ≈ 3 h before measurement. Error bars represent the standard deviation of n = 5 measurement replicates.

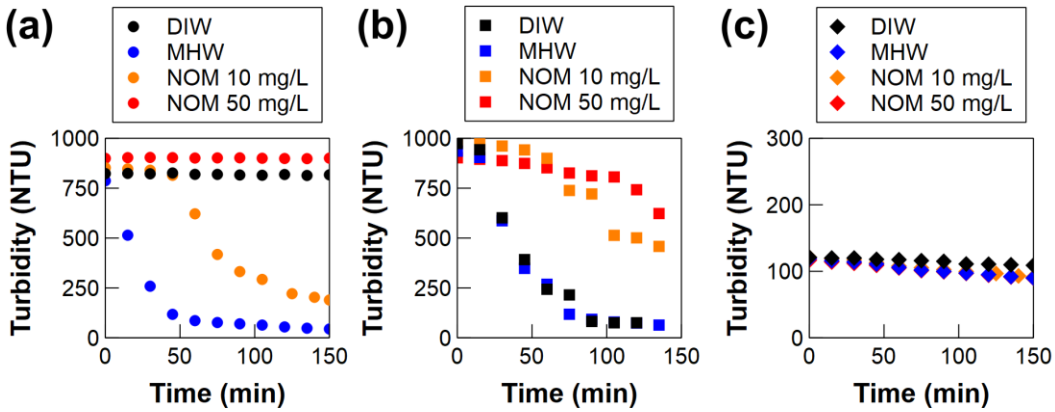

342

343 **Figure 4.** Sedimentation of TiO_2 (a), TiO_2-zeolite composite (b), and zeolite (c) in DIW, MHW,
344 and MHW with NOM. Samples are the same as those measured in Figure 3, with turbidity
345 measurements initiated immediately after preparing the samples.

346

347 Notably, the TiO_2 NPs and the TiO_2-zeolite composites showed opposite trends in
348 degradation efficiency when comparing DIW and MHW backgrounds, with suppressed efficiency
349 of the TiO_2 NPs in MHW relative to DIW, but enhanced efficiency for the composites in MHW
350 (Figure 2). To explain these contradictory results, the effects of water chemistry on both the surface
351 reactivity and aggregation state of the particles (homoaggregation or heteroaggregation) must be
352 considered. In the MHW (pH ≈ 8), the TiO_2 NPs have a near-neutral zeta potential of -0.7 mV
353 (Figure 3). While a stronger negative charge would be expected at pH 8 without electrolytes,[26] the
354 charge is suppressed by charge screening or neutralization by the cations, particularly Ca^{2+}, in the
355 MHW (Ca^{2+} adsorption results discussed *vide infra*). Correspondingly, the diminished electrostatic
356 repulsion resulted in rapid homoaggregation and sedimentation of the TiO_2 NPs in MHW (Figure
357 4a). The zeolite's negative charge is also partially screened or neutralized in the MHW. The surface
358 charge of the composite is between that of the TiO_2 and zeolite in MHW, and there was no
359 significant change in sedimentation rate compared to the composite in DIW (Figure 4b),

suggesting minimal dissociation of the composite (consistent with the TiO_2 having a nearly neutral zeta potential in the MHW, rather than a negative zeta potential that would lead to electrostatic repulsion with the zeolite).

Given the consistent heteroaggregation state of the composite in MHW (0.85 mM $CaCl_2$ + 1.2 mM $NaHCO_3$, pH ≈ 8) and DIW, the composite serves as a useful case to evaluate the role of the water chemistry while maintaining a consistent aggregation state of the TiO_2 NPs. In addition, by using DEET as an uncharged probe compound with no significant difference in adsorption in MHW compared to DIW (SI Figure S1), we are better able to distinguish the effect of water chemistry on surface reactivity independently of differences in probe compound adsorption at different pH that occur in other studies using charged or weak acid/base compounds.[22-24] The results here indicate that the surface reactivity of the TiO_2 is enhanced in MHW. Bicarbonate ions (HCO_3^-) have been reported to scavenge electrons at the TiO_2 surface, thereby extending hole lifetimes to promote surface hydroxyl radical formation[32] and enhance reactivity (particularly at low HCO_3^- concentrations, e.g. < 10 mM),[33] consistent with the results here. In addition, at a higher pH with higher OH^- concentration, hydroxyl radical formation from surface-bound OH^- would be favored,[29] which could potentially result in higher overall reactivity, although prior studies on TiO_2 photocatalysis of other uncharged compounds (e.g. alachlor or chlorfenapyr)[34-36] showed only a small increase in reaction rate upon increasing pH. Therefore, the enhanced reactivity of the composite in MHW is likely more sensitive to the presence of the HCO_3^-.

The reactivity of the TiO_2 NPs alone would also be expected to increase in the MHW, given the same fundamental influences of HCO_3^- and pH noted above. However, the TiO_2 showed a net reduction in efficiency in MHW compared to DIW. This result suggests that the homoaggregation of TiO_2 NPs in MHW has a severely detrimental impact on the reactivity, e.g. by reducing UV

exposure of NPs inside the aggregates, decreasing available surface area for reaction, hindering mass transfer into the aggregates, or increasing hole-electron recombination between particles.[4,5] In contrast, while heteroaggregation can also reduce the reactivity (comparing the composites in DIW to the non-aggregating TiO_2 NPs in DIW), the effect of heteroaggregation appears to be much less detrimental than that of homoaggregation (i.e., the reaction rate is higher for the heteroaggregated composites in MHW than for the homoaggregated TiO_2 NPs in MHW). Hence, a homoaggregation-specific phenomenon such as hole-electron recombination may be predominantly influencing the results for the homoaggregates.

Effect of Zeolite Substrate on NOM Adsorption and Suppression of Photoreactivity

The addition of NOM to the MHW suppressed reactivity of the TiO_2 NPs toward DEET, with a higher degree of suppression observed for the TiO_2 NPs alone than the composites (SI Table S2). While NOM has been reported in some cases enhance photocatalysis, it is more often found to suppress the effective reactivity, e.g., by scavenging holes or reactive oxygen species.[37-42] Here, the difference in the degree of suppression for the TiO_2 alone versus the composites suggests that the total NOM concentration does not completely predict the reactivity. Rather, more detailed information on NOM adsorption onto the NPs may be required. Hence, SEC analyses were conducted to evaluate the adsorption of NOM onto TiO_2, zeolite, and the composites. In SEC, size separation occurs, i.e., larger NOM elutes prior than smaller NOM from ≈ 15 min to 45 min in the chromatograms (Figure 5), and DEET elutes separately after 55 min.

NOM showed the highest adsorption onto the TiO_2 alone, with minimal adsorption to the zeolite alone (Figure 5). Even more notable, the SEC results indicate that the presence of the zeolite substrate in the composites substantially discourages NOM adsorption to the TiO_2 NPs, despite

containing the same NP concentration as the TiO_2 alone. As such, the degree of suppression of the TiO_2 reactivity toward DEET showed a good correlation with the adsorbed NOM concentration (rather than the dissolved or total NOM) across all samples (SI Figure S4). It was noted that the DEET does not show any strong complexation with the dissolved NOM that would influence its adsorption or reactivity (SI Figure S5). The SEC analysis also showed loss of the bulk NOM over the photoreaction experiments (SI Figure S6), suggesting that NOM continually adsorbs and degrades, competing with DEET for reaction with ROS at or near the TiO_2 surface.

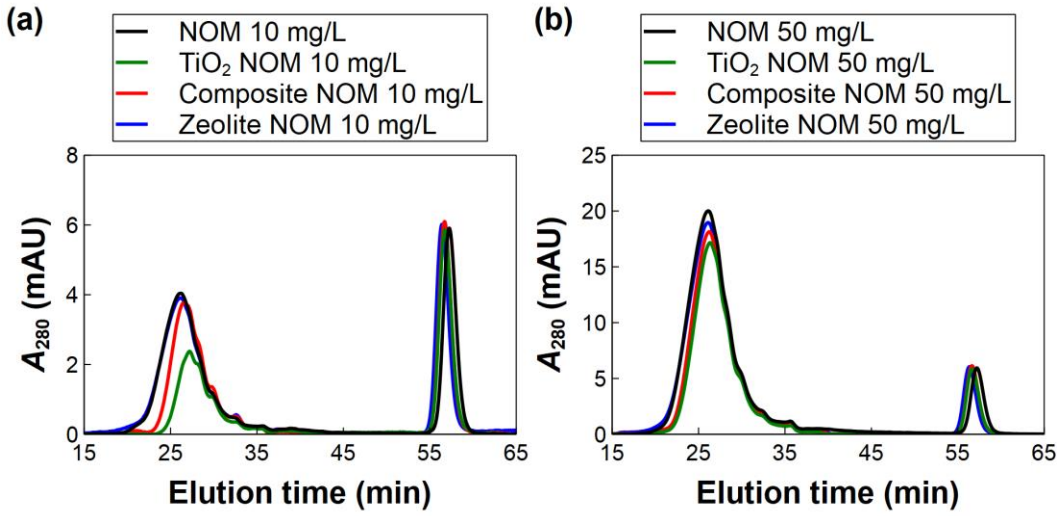

Figure 5. SEC with UV detection at 280 nm for 10 mg/L of NOM (a) and 50 mg/L of NOM (b), before (black lines) and after adsorption from MHW onto TiO_2 nanoparticles alone (0.2 g/L), TiO_2-zeolite composites (0.2 g/L TiO_2 + 0.6 g/L zeolite), and zeolite particles alone (0.6 g/L). All samples included 50 mg/L of free DEET, after accounting for DEET adsorption to the zeolite (i.e., zeolite-containing samples had a total concentration of 100 mg/L of DEET initially added). Samples were collected from dark (foil-wrapped) controls that were run in parallel with the photoreaction experiments, centrifuged to remove particles, and filtered through 0.2 μm nylon syringe filters prior to SEC analysis.

We hypothesize that the diminished adsorption of NOM onto the composites could result from strong electrostatic repulsion of the NOM by the negatively-charged zeolite substrate, and/or depletion of Ca^{2+} from the MHW background onto zeolite, reducing the Ca^{2+} available to bridge NOM to the TiO_2. The possibility for electrostatic interactions (i.e., zeolite–NOM charge repulsion) to influence the NOM adsorption independently of any Ca^{2+} bridging effects was evaluated by replacing the Ca^{2+} in MHW with the same molar equivalents of Na^+, i.e., [NaCl] = 2[$CaCl_2$] = 1.7 mM. After eliminating the Ca^{2+}, a slightly lower adsorption from 10 mg/L NOM was observed on the composite than the TiO_2 (SI Figure S7a), suggesting electrostatic repulsion by the zeolite substrate can influence NOM adsorption onto the attached TiO_2 NPs. However, samples without Ca^{2+} showed much lower NOM adsorption overall than those with Ca^{2+}, emphasizing the greater importance of Ca^{2+} bridging. The adsorption of Ca^{2+} onto the particles was then evaluated by measuring the concentration of free Ca^{2+} remaining after 1 h equilibration of the various particle types in the MHW. The TiO_2 alone and zeolite alone showed similar Ca^{2+} adsorption at the particle concentrations used: 54% ± 3% and 53% ± 1% of the 0.85 mM of total Ca^{2+} was adsorbed onto the TiO_2 and zeolite, respectively (n = 3 measurement replicates per sample). The lack of bridging adsorption of NOM onto the zeolite despite the Ca^{2+} adsorption could be attributable to electrostatic repulsion by the zeolite or perhaps Ca^{2+} adsorbing within pore spaces in the zeolite that are inaccessible to the NOM. In the composite, a similar level of Ca^{2+} adsorption (56% ± 3%, n = 3) was again observed to the two materials alone, and the NOM adsorption onto the composite was intermediate between that on the TiO_2 and zeolite alone. The fact that Ca^{2+} adsorption from the two independent particles is not additive in the composite suggests that the zeolite and TiO_2 in the composite are competing for the Ca^{2+} ions. Hence, the

presence of the zeolite substrate reduces the Ca^{2+} available to bridge NOM onto the TiO_2 surface, resulting in lower NOM attachment and higher effective reactivity of the TiO_2 toward DEET.

In addition to the effect of the adsorbed NOM on the degradation efficiency, the effects of NOM on the particle stability or aggregation state were assessed. As shown in Figure 3, the addition of NOM caused the TiO_2 surface charge to become more negative. The NOM can therefore impart both electrostatic and steric repulsion forces to enhance the colloidal stability of the particles. The TiO_2 NPs indeed showed delayed settling in the presence of 10 mg/L of NOM and no sedimentation after 2.5 h in 50 mg/L of NOM (Figure 4a). The DLS measurements taken at the end of the photoreaction experiments also showed improved NP stability in 50 mg/L of NOM (d_z = 311 ± 4 nm in dark conditions) compared to MHW without NOM, although extensive aggregation (d_z >> 1 μm) occurred after UV exposure with 50 mg/L of NOM or in 10 mg/L of NOM under both UV and dark conditions. The composites were also found to settle increasingly slowly as the NOM concentration increased (Figure 4b), indicating that the addition of NOM causes the composites to partially disaggregate.

As a robust composite is desirable to allow separation of the NPs from the treated water, this form of electrostatically-bound composite would thus have limited utility for treatment of NOM-containing waters. From a more fundamental perspective, disaggregation of the TiO_2 NPs on its own would be expected to improve reactivity (as seen in media without NOM), but here the positive effects of disaggregation are relatively insignificant compared to the substantial suppression of reactivity upon surface fouling of the TiO_2 NPs by NOM. Therefore, strategies to achieve the highest efficiency for water treatment should foremost prioritize approaches to mitigate NOM adsorption, followed by approaches to mitigate homoaggregation. The results here suggest that both goals can be achievable by tuning the substrate used for immobilization.

DEET Byproduct Formation and Reaction Pathways

The degradation of a parent compound can involve its transformation to several intermediates before complete mineralization to carbon dioxide is achieved. The intermediate products formed in the reaction pathway might have toxicity and chemical properties different from that of the parent compound. Hence, the treated water should be analyzed for the presence of byproducts. Byproduct analysis can also be used to identify more subtle influences of the reaction conditions on the degradation pathway, beyond the analysis of solely the DEET removal rate. In this study, we apply byproduct analysis to evaluate whether the DEET adsorbed to the zeolite in the composites remains susceptible to degradation by the TiO_2 NPs, and whether the reaction pathway is influenced by the aggregation state or water chemistry.

Prior DEET degradation studies using TiO_2 NPs for photocatalysis have identified the presence of several common intermediates.[43,44] Figure 6 shows the initial stages of DEET byproduct formation and degradation.[43,45] To our knowledge, no DEET degradation studies thus far have compared byproduct formation when using a composite material versus TiO_2 NPs alone. Here, intermediate products were first putatively identified by molecular feature extraction on the MS scan data, followed by molecular formula generation for each compound discovered using the high-resolution TOF data (MassHunter Qualitative software, v. 10.0, Agilent Technologies). Then, the QTOF MS/MS data (collected in All Ions mode) were used to obtain the fragmentation patterns of the compounds, which were compared to those reported by Medana et al. to assign the identification of the byproducts.[45]

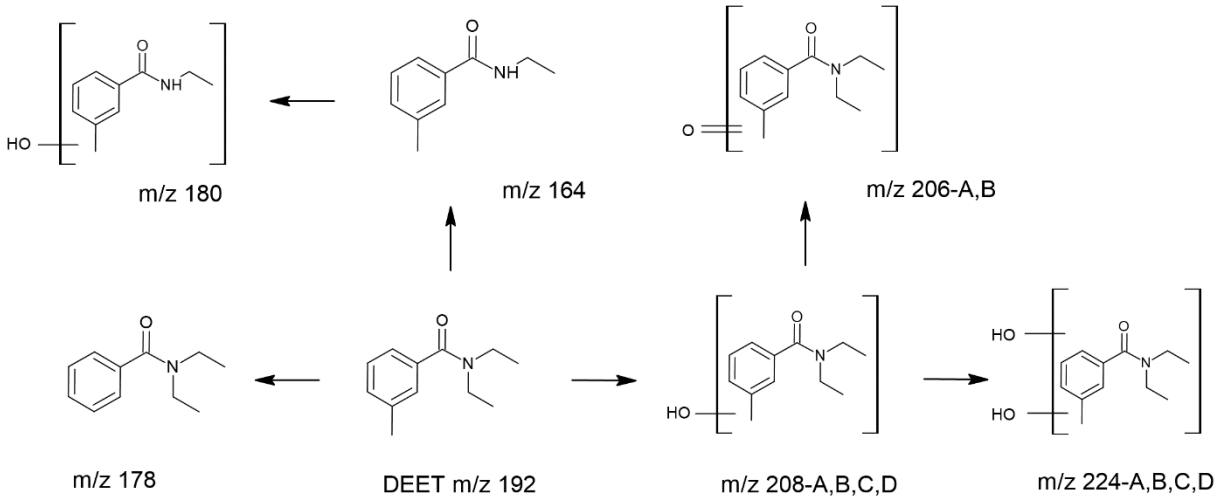

Figure 6. Reaction pathway for early-stage photocatalytic degradation of DEET. For isomer structures (A,B,C,D) and further degradation pathways, the reader is referred to Medana et al.[45]

The DEET degradation pathway is generally reported to involve the transformation of the aromatic ring or alkyl chains of DEET by the attack of hydroxyl radical. The *m*/*z* 164 byproduct, *N*-ethyl-*m*-toluamide, forms by breaking the C-N bond to abstract one ethyl group,[45,46] while the *m*/*z* 178 product forms by the removal of the methyl group from the aromatic ring of DEET.[45] Alternatively, hydroxyl radical attack to add hydroxyl groups results in the formation of mono- and bi-hydroxylated compounds (*m*/*z* 208 and 224) or higher order hydroxylated byproducts (not shown in Figure 6).[44] Several isomers can be formed, which vary based on the location of OH addition onto either the aromatic ring or the methyl group and can be inferred from the fragmentation pattern.[45] The alcohol group in the *m*/*z* 208 byproducts can further be oxidized to an aldehyde group to form the *m*/*z* 206 byproduct.

In this study, byproducts with *m*/*z* of 164, 208, 206, and 224 were observed with relatively strong UV signals (example chromatogram in SI Figure S8; retention times in SI Table S4). Quantitative analysis of the byproducts was accomplished using the UV chromatograms, with

QTOF analysis only to confirm the byproducts rather than for quantitation (no internal standards were included to correct for drift or other variability in the QTOF measurements). The MS/MS fragmentation results for the *m*/*z* 208, 206, and 224 byproducts (SI Figure S9) suggest the intermediates to be the isomers 208-C/D, 206-A, and 224-A as reported by Medana et al.,[45] with the OH groups on the aromatic ring for 208-C/D and 224-A (i.e., no hydroxylation of the methyl group).[45] Many other byproducts were also present, but here we focus on only three early-stage products with relatively well-defined UV peaks. For example, the *m*/*z* 178 byproduct was observed but not evaluated due to incomplete chromatographic separation from other peaks. Because raw UV peak areas are difficult to compare meaningfully across samples with different DEET decay rates, the UV area of the byproducts was normalized by the concentration of DEET degraded at each time point, somewhat akin to a stoichiometric analysis of products formed per DEET reactant.

The quantitative byproduct analyses are presented in Figures 7, 8, S9, and S10. Comparing TiO_2 alone to the composite, the byproduct analysis showed that despite adding a higher initial concentration of DEET to the composites (100 mg/L, compared to 50 mg/L for TiO_2 only), no large increase in formation of the initial byproducts (*m*/*z* 164 and 208) was observed for the composites (Figures 7 and 8). That is, the 50 mg/L of DEET adsorbed by the zeolites appears to be strongly adsorbed (minimal diffusion across the zeolite toward the TiO_2 NPs[7]) and inaccessible to photocatalytic degradation, as it did not release any additional byproducts into the solution. The byproduct profiles over time also showed similar trends between the two materials: the *m*/*z* 164 byproduct, *N*-ethyl-*m*-toluamide, was readily formed and easily degraded, and the bihydroxylated product (*m*/*z* 224) appears to form subsequently to the monohydroxylated DEET derivative (*m*/*z* 208), consistent with the pathway in Figure 6. These similarities suggest that heteroaggregation of the TiO_2 onto the zeolite does not significantly influence the reaction pathway.

Interestingly, the presence of high adsorbed amounts of NOM (in 50 mg/L of NOM for the composites, or 10 or 50 mg/L of NOM for the TiO_2 alone) resulted in higher levels of the *m*/*z* 164 byproduct but lower levels of *m*/*z* 208 (and subsequent byproducts, *m*/*z* 224 and 206) at the initial time points (up to 15 min), relative to MHW without NOM. This phenomenon could suggest that the adsorbed NOM favors de-ethylation of the tertiary amide to form *m*/*z* 164 over hydroxylation of the DEET to the *m*/*z* 208 byproduct. These results are consistent with suppressed hydroxylation pathways reported for ciprofloxacin and sulfamethoxazole photocatalysis by TiO_2 in the presence of NOM and suggest hydroxyl radical scavenging by the NOM.[42,47] Alternatively, the NOM may suppress the subsequent degradation of *m*/*z* 164 more effectively than *m*/*z* 208, or otherwise show a different interaction (e.g. sorption) with the two byproducts. However, as the mixture of DEET degradation byproducts has been reported to have lower toxicity than the initial DEET solution,[45] differences in the reaction pathway for this compound may have little practical effect on the safety of the treated water.

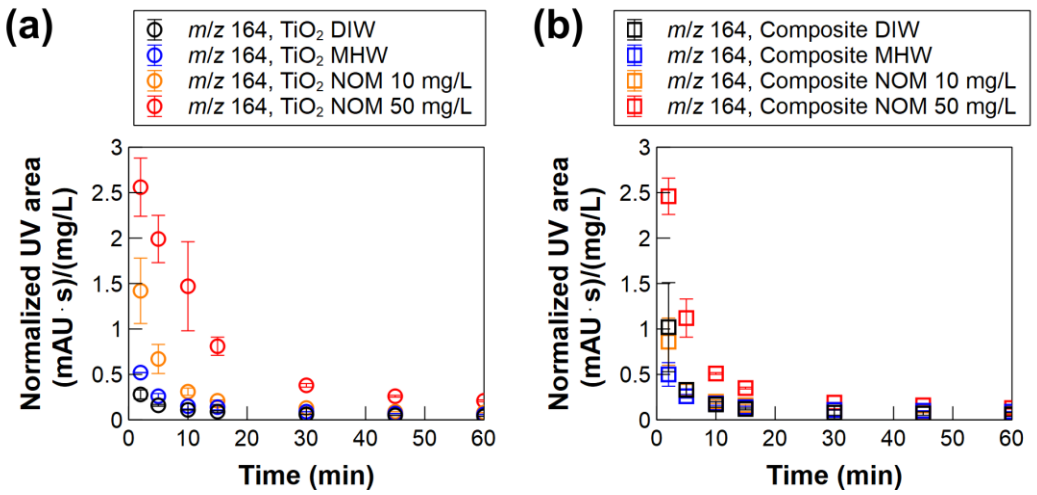

Figure 7. Normalized UV peak area of the de-ethylation byproduct (*m*/*z* 164) using TiO_2 NPs (a) and TiO_2-zeolite composites (b) in DIW, MHW, 10 mg/L NOM, and 50 mg/L NOM. Adsorption

548 of NOM to the TiO_2 appears to promote this byproduct formation pathway. Samples are the same
549 as those shown in Figure 2; byproducts are identified in the chromatogram in SI Figure S8 with
550 structures shown in Figure 6. Error bars represent the standard deviation of at least two
551 experimental replicates.
552

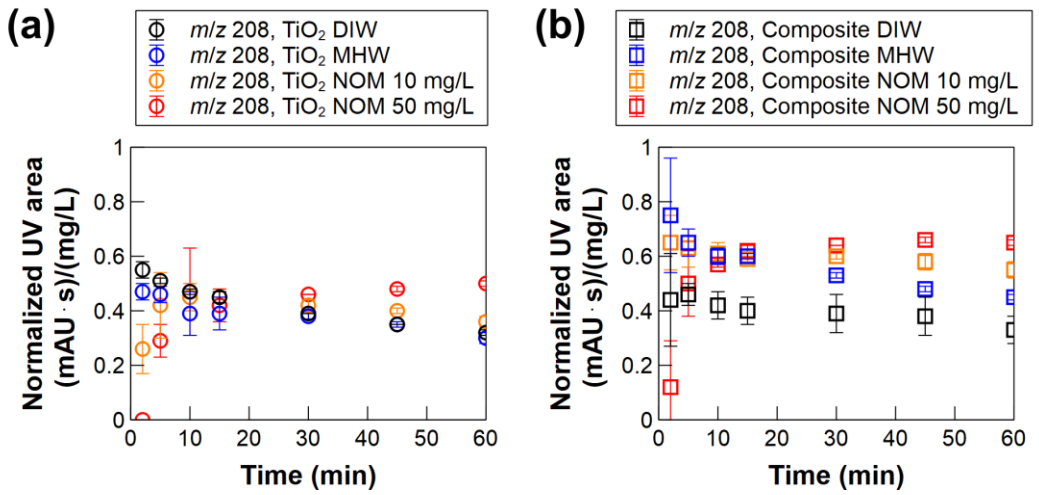

553

554 **Figure 8**. Normalized UV peak area of the monohydroxylation byproduct (*m*/*z* 208) using TiO_2
555 NPs (a) and TiO_2-zeolite composites (b) in DIW, MHW, 10 mg/L NOM, and 50 mg/L NOM.
556 Adsorption of NOM to the TiO_2 appears to demote this byproduct formation pathway. Samples
557 are the same as those shown in Figure 2; byproducts are identified in the chromatogram in SI
558 Figure S8 with structures shown in Figure 6. Error bars represent the standard deviation of at least
559 two experimental replicates. Similar analyses of two subsequent byproducts of *m*/*z* 208 are
560 reported in the SI Figures S10 and S11.
561

562 **Conclusions**

563 This study provides a systematic analysis of the role of a zeolite substrate and water
564 chemistry on the photocatalytic efficiency of TiO_2 nanoparticles for removal of DEET. It also

provides insight into the impacts of homoaggregation, heteroaggregation (or immobilization onto a substrate), water chemistry, and NOM surface fouling on the reactivity of TiO_2 NPs, as summarized in Figure 9. These processes were found to have different relative levels of importance to the photocatalytic efficiency of TiO_2 NPs: NOM adsorption had the strongest influence on the reactivity of TiO_2 NPs, followed by the homoaggregation of the NPs, the electrolyte composition and pH of the medium (specifically comparing MHW and DIW here), and the heteroaggregation of the NPs having the least effect.

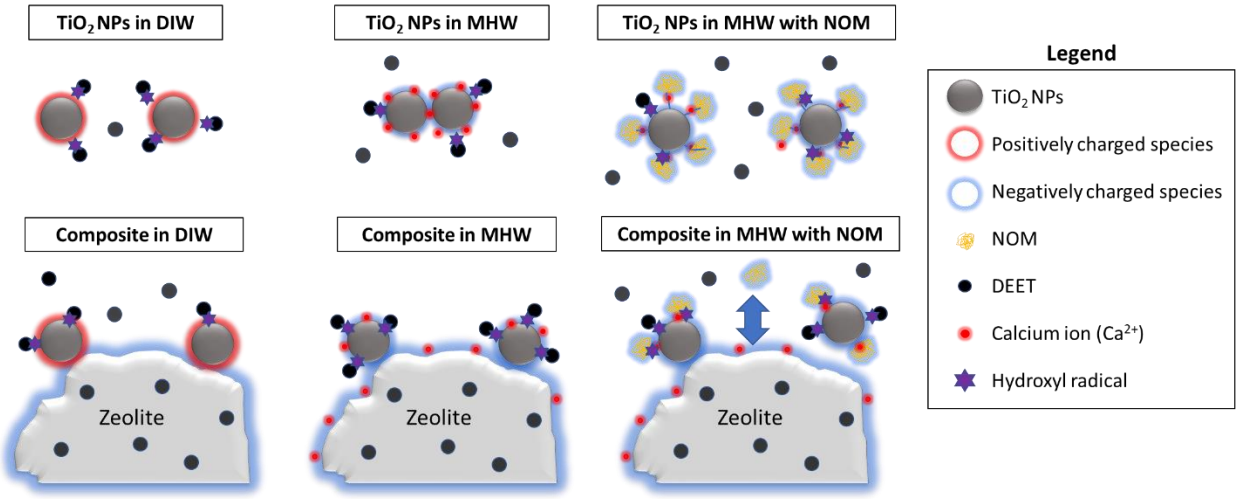

Figure 9. Summary of changes in the reactivity of TiO_2 NPs toward DEET upon heteroaggregation to form TiO_2-zeolite composites, homoaggregation in MHW, and surface fouling by NOM (which is mitigated by Ca^{2+} depletion onto the zeolite).

Notably, the zeolite substrate could enhance the performance of the TiO_2 for DEET degradation by reducing NOM adsorption (primarily via depletion of the Ca^{2+} available for bridging), as well as by preventing homoaggregation of the TiO_2 NPs (such that the reactivity was enhanced in MHW, where the pure TiO_2 suspension rapidly homoaggregates). The zeolite can also adsorb DEET, although this adsorption capacity would eventually be depleted since the DEET is

582 sequestered in an unreactive state. The application of advanced characterization methods (SEC
583 and QTOF MS) enabled fundamental insights into the role of the adsorbed NOM (as opposed to
584 bulk NOM) and mechanisms for the substrate to influence NOM adsorption to the TiO_2, as well
585 as the influence of the NOM on the DEET byproduct formation pathways. As a number of
586 biomolecules, such as proteins and amino acids, can also adsorb to TiO_2,[48-53] the generalizability
587 of the results for NOM to other coatings or the influence of the substrate on competitive adsorption
588 processes[27,52] can also be interesting to investigate in future studies.

589 Overall, the combined understanding of the role of substrate and water chemistry identified
590 in this study highlights key factors that influence the performance of photocatalytic nanomaterials
591 for water treatment applications. The primary limitation of the TiO_2-zeolite composite tested here
592 is the poor robustness of the NP attachment to the zeolite in the presence of NOM. This limitation
593 may be overcome by using other synthesis routes, e.g. sol-gel synthesis of the NPs in the presence
594 of the zeolite followed by calcination; however, if the TiO_2 forms a more homogeneous film
595 coating over the zeolite, the blocking of the zeolite surface may counter some of the unique benefits
596 conferred by the substrate, as identified here.

597 More broadly, heteroaggregation is a commonly occurring phenomenon that will also
598 occur upon incidental release of NPs into natural environments. Many environmental
599 heteroaggregation studies have focused on methods to measure heteroaggregation and the
600 implications for NP fate and transport,[28,54-60] while few have investigated the effects on the
601 photocatalytic reactivity of the NPs. This study demonstrates one specific case in which
602 heteroaggregation may result in a net higher reactivity by mitigating homoaggregation and fouling
603 by NOM. Future studies should explore the generalizability of the results here for zeolite to other
604 potential substrates.

Supplementary Information

Additional method information, DEET removal rate analyses, SEC analyses, and QTOF analyses are provided in the Supplementary Information.

Acknowledgements

This material is based upon work supported by the National Science Foundation under Grant No. 1705511. We thank Prof. Devin Shaffer for use of the turbidimeter, Mr. Howard Louie for assistance with installation of the QTOF nitrogen generator and uninterruptible power supply, Prof. Greg Lowry for the SEC column, Evonik Industries for providing the Aeroxide TiO_2 P25 nanoparticles, and Dr. Charisma Lattao for general laboratory assistance.

Conflicts of Interest

There are no conflicts of interest to declare.

References

1. B. C. Hodges, E. L. Cates and J.-H. Kim, Challenges and prospects of advanced oxidation water treatment processes using catalytic nanomaterials, *Nat. Nanotechnol.*, 2018, **13**, 642-650.
2. K. Guesh, C. Márquez-Álvarez, Y. Chebude and I. Díaz, Enhanced photocatalytic activity of supported TiO_2 by selective surface modification of zeolite Y, *Appl. Surf. Sci.*, 2016, **378**, 473-478.
3. H. Dong, G. Zeng, L. Tang, C. Fan, C. Zhang, X. He and Y. He, An overview on limitations of TiO_2-based particles for photocatalytic degradation of organic pollutants and the corresponding countermeasures, *Water Res.*, 2015, **79**, 128-146.
4. D. Jassby, J. Farner Budarz and M. Wiesner, Impact of aggregate size and structure on the photocatalytic properties of TiO_2 and ZnO nanoparticles, *Environ. Sci. Technol.*, 2012, **46**, 6934-6941.
5. J. Sun, L.-H. Guo, H. Zhang and L. Zhao, UV irradiation induced transformation of TiO_2 nanoparticles in water: Aggregation and photoreactivity, *Environ. Sci. Technol.*, 2014, **48**, 11962-11968.
6. D. Martel, A. Guerra, P. Turek, J. Weiss and B. Vileno, Pertinent parameters in photo-generation of electrons: Comparative study of anatase-based nano-TiO_2 suspensions, *J. Colloid Interface Sci.*, 2016, **467**, 300-306.
7. O. Carp, C. L. Huisman and A. Reller, Photoinduced reactivity of titanium dioxide, *Prog. Solid State Chem.*, 2004, **32**, 33-177.
8. M. Cargnello, T. R. Gordon and C. B. Murray, Solution-phase synthesis of titanium dioxide nanoparticles and nanocrystals, *Chem. Rev.*, 2014, **114**, 9319-9345.
9. P. Munnik, P. E. de Jongh and K. P. de Jong, Recent developments in the synthesis of supported catalysts, *Chem. Rev.*, 2015, **115**, 6687-6718.
10. Y. Xu and C. H. Langford, Photoactivity of titanium dioxide supported on MCM41, zeolite X, and zeolite Y, *J. Phys. Chem. B*, 1997, **101**, 3115-3121.
11. P. Fu, Y. Luan and X. Dai, Preparation of activated carbon fibers supported TiO_2 photocatalyst and evaluation of its photocatalytic reactivity, *J. Mol. Catal. A: Chem.*, 2004, **221**, 81-88.
12. S. Yao, J. Li and Z. Shi, Immobilization of TiO_2 nanoparticles on activated carbon fiber and its photodegradation performance for organic pollutants, *Particuology*, 2010, **8**, 272-278.
13. N. X. D. Mai, J. Bae, I. T. Kim, S. H. Park, G.-W. Lee, J. H. Kim, D. Lee, H. B. Son, Y.-C. Lee and J. Hur, A recyclable, recoverable, and reformable hydrogel-based smart photocatalyst, *Environ. Sci.: Nano*, 2017, **4**, 955-966.
14. A. Martucci, L. Pasti, N. Marchetti, A. Cavazzini, F. Dondi and A. Alberti, Adsorption of pharmaceuticals from aqueous solutions on synthetic zeolites, *Microporous Mesoporous Mater.*, 2012, **148**, 174-183.
15. Y.-H. Jan, L.-Y. Lin, M. Karthik and H. Bai, Titanium dioxide/zeolite catalytic adsorbent for the removal of NO and acetone vapors, *J. Air Waste Manage. Assoc.*, 2009, **59**, 1186-1193.
16. I. Jansson, S. Suárez, F. J. Garcia-Garcia and B. Sánchez, Zeolite–TiO_2 hybrid composites for pollutant degradation in gas phase, *Appl. Catal., B*, 2015, **178**, 100-107.

17. D. Kanakaraju, J. Kockler, C. A. Motti, B. D. Glass and M. Oelgemoller, Titanium dioxide/zeolite integrated photocatalytic adsorbents for the degradation of amoxicillin, *Appl. Catal., B*, 2015, **166-167**, 45-55.
18. M. Lafjah, F. Djafri, A. Bengueddach, N. Keller and V. Keller, Beta zeolite supported sol–gel TiO_2 materials for gas phase photocatalytic applications, *J. Hazard. Mater.*, 2011, **186**, 1218-1225.
19. S. Sampath, H. Uchida and H. Yoneyama, Photocatalytic degradation of gaseous pyridine over zeolite-supported titanium dioxide, *J. Catal.*, 1994, **149**, 189-194.
20. G. Zhang, A. Song, Y. Duan and S. Zheng, Enhanced photocatalytic activity of TiO_2/zeolite composite for abatement of pollutants, *Microporous Mesoporous Mater.*, 2018, **255**, 61-68.
21. *U.S. Pat.*, 9,290,394 B2, 2016.
22. K. M. Reza, A. S. W. Kurny and F. Gulshan, Parameters affecting the photocatalytic degradation of dyes using TiO_2: a review, *Appl. Water Sci.*, 2017, **7**, 1569-1578.
23. U. G. Akpan and B. H. Hameed, Parameters affecting the photocatalytic degradation of dyes using TiO_2-based photocatalysts: A review, *J. Hazard. Mater.*, 2009, **170**, 520-529.
24. I. K. Konstantinou and T. A. Albanis, TiO_2-assisted photocatalytic degradation of azo dyes in aqueous solution: kinetic and mechanistic investigations: A review, *Appl. Catal., B*, 2004, **49**, 1-14.
25. D. E. Curry, K. A. Andrea, A. J. Carrier, C. Nganou, H. Scheller, D. Yang, B. Youden, Y. Zhang, A. Nicholson, S. Cui, K. D. Oakes, S. L. MacQuarrie, M. Lu and X. Zhang, Surface interaction of doxorubicin with anatase determines its photodegradation mechanism: insights into removal of waterborne pharmaceuticals by TiO_2 nanoparticles, *Environ. Sci.: Nano*, 2018, **5**, 1027-1035.
26. National Institute of Standards and Technology, *SRM 1898 Titanium Dioxide Nanomaterial*, Gaithersburg, MD, 2012.
27. S. Shakiba, A. Hakimian, L. R. Barco and S. M. Louie, Dynamic intermolecular interactions control adsorption from mixtures of natural organic matter and protein onto titanium dioxide nanoparticles, *Environ. Sci. Technol.*, 2018, **52**, 14158-14168.
28. A. Praetorius, E. Badetti, A. Brunelli, A. Clavier, J. A. Gallego-Urrea, A. Gondikas, M. Hassellöv, T. Hofmann, A. Mackevica, A. Marcomini, W. Peijnenburg, J. T. K. Quik, M. Seijo, S. Stoll, N. Tepe, H. Walch and F. von der Kammer, Strategies for determining heteroaggregation attachment efficiencies of engineered nanoparticles in aquatic environments, *Environ. Sci.: Nano*, 2020, **7**, 351-367.
29. C. S. Turchi and D. F. Ollis, Photocatalytic degradation of organic water contaminants: Mechanisms involving hydroxyl radical attack, *J. Catal.*, 1990, **122**, 178-192.
30. D. F. Ollis, Kinetics of liquid phase photocatalyzed reactions: An illuminating approach, *J. Phys. Chem. B*, 2005, **109**, 2439-2444.
31. D. F. Ollis, Kinetics of photocatalyzed reactions: Five lessons learned, *Front. Chem.*, 2018, **6**.
32. A. Molinari, L. Samiolo and R. Amadelli, EPR spin trapping evidence of radical intermediates in the photo-reduction of bicarbonate/CO_2 in TiO_2 aqueous suspensions, *Photochem. Photobiol. Sci.*, 2015, **14**, 1039-1046.
33. J. Farner Budarz, A. Turolla, A. F. Piasecki, J.-Y. Bottero, M. Antonelli and M. R. Wiesner, Influence of aqueous inorganic anions on the reactivity of nanoparticles in TiO_2 photocatalysis, *Langmuir*, 2017, **33**, 2770-2779.

34. C. C. Wong and W. Chu, The direct photolysis and photocatalytic degradation of alachlor at different TiO_2 and UV sources, *Chemosphere*, 2003, **50**, 981-987.
35. W. Chu and C. C. Wong, Study of herbicide alachlor removal in a photocatalytic process through the examination of the reaction mechanism, *Ind. Eng. Chem. Res.*, 2004, **43**, 5027-5031.
36. Y. Cao, J. Chen, L. Huang, Y. Wang, Y. Hou and Y. Lu, Photocatalytic degradation of chlorfenapyr in aqueous suspension of TiO_2, *J. Mol. Catal. A: Chem.*, 2005, **233**, 61-66.
37. C. S. Uyguner-Demirel, N. C. Birben and M. Bekbolet, Elucidation of background organic matter matrix effect on photocatalytic treatment of contaminants using TiO_2: A review, *Catal. Today*, 2017, **284**, 202-214.
38. M. Ren, M. Drosos and F. H. Frimmel, Inhibitory effect of NOM in photocatalysis process: Explanation and resolution, *Chem. Eng. J.*, 2018, **334**, 968-975.
39. M. Drosos, M. Ren and F. H. Frimmel, The effect of NOM to TiO_2: interactions and photocatalytic behavior, *Appl. Catal., B*, 2015, **165**, 328-334.
40. Y. Ye, H. Bruning, W. Liu, H. Rijnaarts and D. Yntema, Effect of dissolved natural organic matter on the photocatalytic micropollutant removal performance of TiO_2 nanotube array, *J. Photochem. Photobiol., A*, 2019, **371**, 216-222.
41. J. R. Garbin, D. M. B. P. Milori, M. L. Simões, W. T. L. da Silva and L. M. Neto, Influence of humic substances on the photolysis of aqueous pesticide residues, *Chemosphere*, 2007, **66**, 1692-1698.
42. S. Li and J. Hu, Transformation products formation of ciprofloxacin in UVA/LED and UVA/LED/TiO_2 systems: Impact of natural organic matter characteristics, *Water Res.*, 2018, **132**, 320-330.
43. F. J. Benitez, J. L. Acero, F. J. Real, G. Roldan and E. Rodriguez, Photolysis of model emerging contaminants in ultra-pure water: Kinetics, by-products formation and degradation pathways, *Water Res.*, 2013, **47**, 870-880.
44. E. Mena, A. Rey, E. M. Rodríguez and F. J. Beltrán, Reaction mechanism and kinetics of DEET visible light assisted photocatalytic ozonation with WO_3 catalyst, *Appl. Catal., B*, 2017, **202**, 460-472.
45. C. Medana, P. Calza, F. Bello, E. Raso, C. Minero and C. Baiocchi, Multiple unknown degradants generated from the insect repellent DEET by photoinduced processes on TiO_2, *J. Mass Spectrom.*, 2011, **46**, 24-40.
46. Z. Yu, Y. Sun, G. Zhang and C. Zhang, Degradation of DEET in aqueous solution by water falling film dielectric barrier discharge：Effect of three operating modes and analysis of the mechanism and degradation pathway, *Chem. Eng. J.*, 2017, **317**, 90-102.
47. R. Yuan, Y. Zhu, B. Zhou and J. Hu, Photocatalytic oxidation of sulfamethoxazole in the presence of TiO_2: Effect of matrix in aqueous solution on decomposition mechanisms, *Chem. Eng. J.*, 2019, **359**, 1527-1536.
48. J. Kim and K. Doudrick, Emerging investigator series: protein adsorption and transformation on catalytic and food-grade TiO_2 nanoparticles in the presence of dissolved organic carbon, *Environ. Sci.: Nano*, 2019, **6**, 1688-1703.
49. B. E. Givens, Z. Xu, J. Fiegel and V. H. Grassian, Bovine serum albumin adsorption on SiO_2 and TiO_2 nanoparticle surfaces at circumneutral and acidic pH: A tale of two nano-bio surface interactions, *J. Colloid Interface Sci.*, 2017, **493**, 334-341.

50. I. Sit, Z. Xu and V. H. Grassian, Plasma protein adsorption on TiO_2 nanoparticles: Impact of surface adsorption on temperature-dependent structural changes, *Polyhedron*, 2019, **171**, 147-154.
51. I. B. Ustunol, N. I. Gonzalez-Pech and V. H. Grassian, pH-dependent adsorption of α-amino acids, lysine, glutamic acid, serine and glycine, on TiO_2 nanoparticle surfaces, *J. Colloid Interface Sci.*, 2019, **554**, 362-375.
52. H. Wu, N. I. Gonzalez-Pech and V. H. Grassian, Displacement reactions between environmentally and biologically relevant ligands on TiO_2 nanoparticles: insights into the aging of nanoparticles in the environment, *Environ. Sci.: Nano*, 2019, **6**, 489-504.
53. Z. Xu and V. H. Grassian, Bovine serum albumin adsorption on TiO_2 nanoparticle surfaces: Effects of pH and coadsorption of phosphate on protein–surface interactions and protein structure, *J. Phys. Chem. C*, 2017, **121**, 21763-21771.
54. L. E. Barton, M. Therezien, M. Auffan, J.-Y. Bottero and M. R. Wiesner, Theory and methodology for determining nanoparticle affinity for heteroaggregation in environmental matrices using batch measurements, *Environ. Eng. Sci.*, 2014, **31**, 421-427.
55. J. Labille, C. Harns, J.-Y. Bottero and J. Brant, Heteroaggregation of titanium dioxide nanoparticles with natural clay colloids, *Environ. Sci. Technol.*, 2015, **49**, 6608-6616.
56. A. Praetorius, J. Labille, M. Scheringer, A. Thill, K. Hungerbühler and J.-Y. Bottero, Heteroaggregation of titanium dioxide nanoparticles with model natural colloids under environmentally relevant conditions, *Environ. Sci. Technol.*, 2014, **48**, 10690-10698.
57. H. Wang, Y.-n. Dong, M. Zhu, X. Li, A. A. Keller, T. Wang and F. Li, Heteroaggregation of engineered nanoparticles and kaolin clays in aqueous environments, *Water Res.*, 2015, **80**, 130-138.
58. B. M. Smith, D. J. Pike, M. O. Kelly and J. A. Nason, Quantification of heteroaggregation between citrate-stabilized gold nanoparticles and hematite colloids, *Environ. Sci. Technol.*, 2015, **49**, 12789-12797.
59. M. C. Surette and J. A. Nason, Nanoparticle aggregation in a freshwater river: the role of engineered surface coatings, *Environ. Sci.: Nano*, 2019, **6**, 540-553.
60. N. K. Geitner, N. J. O'Brien, A. A. Turner, E. J. Cummins and M. R. Wiesner, Measuring nanoparticle attachment efficiency in complex systems, *Environ. Sci. Technol.*, 2017, **51**, 13288-13294.